

Aerodynamic Analysis of a Vertical Axis Wind Turbine in a Diffuser

Ben Geurts

B.M.Geurts@tudelft.nl

Carlos Simão Ferreira

C.J.SimaoFerreira@tudelft.nl

Gerard van Bussel

G.J.W.vanBussel@tudelft.nl

DUWIND

Delft University of Technology

Kluyverweg 1

2629HS Delft

The Netherlands

Abstract

Wind energy in the urban environment faces complex and often unfavorable wind conditions. High turbulence, lower average wind velocities and rapid changes in the wind direction are common phenomena in the complex built environments. A possible way to improve the cost-efficiency of urban wind turbines is the application of flow-enhancing structures on or near the turbines. For horizontal axis wind turbines (HAWTs), applying a diffuser has shown to have a beneficial impact on the power production, but it is still under development. For a vertical axis wind turbine (VAWT) it is expected that flow augmentation will also strongly increase the performance of the turbine, but very little research has been done in this field. The purpose of this research is to investigate the effects of a diffuser on the airflow through a VAWT. In order to investigate these effects, the turbine (with and without diffuser) is simulated using a 2-D unsteady free-wake potential-flow panel model. The local flow field, local angles of attack, shed vorticity, the shape and strength of the wake, and the rotor torque are investigated for both the case with and without the diffuser. The diffuser used in this research consists of two mirrored airfoil cross-sections. The size of the duct-opening in which the turbine operates is varied. This work shows that unlike for a 1-D actuator disc analysis, the area ratio β of the diffuser exit with respect to the diffuser nozzle area is not the only driving factor in the augmentation of the rotor torque of the VAWT. More important are the effect of the directional change of the rotor inflow and the faster downstream transport of the shed vorticity.

1 The Operation of Diffuser-augmented Wind Turbines (DAWTs)

The amount of energy that can be extracted by a HAWT is expressed as the non-dimensional power coefficient C_P . It is the ratio between the kinetic power which is contained in the free-stream wind and the amount of energy that is eventually converted by the wind turbine. HAWTs can be modeled in a very simplistic way as actuator discs in a quasi 1-dimensional flow. This actuator disc model shows that the maximum obtainable power coefficient is 0.59. This theoretical maximum is obtained when the axial induction factor a is equal to $1/3$. In this situation the flow is decelerated to $2/3$ and $1/3$ of its original free-stream velocity at the rotor-disc and in the far wake respectively. As explained by Van Bussel [3],[4], this same ratio also applies to a diffuser-augmented wind turbine (DAWT) as long as the diffuser does not induce a (negative) back-pressure. In this analogy with unaugmented turbines, the flow deceleration of $1/3$ is now assumed to occur at the exit of the diffuser and can be expressed as in equation 1. With this same velocity reduction ratio, the power increase due to the diffuser is purely a result of the increased mass flow through the rotor-disc. The area of the rotor-disc remains the same, but as a result of the diffuser, the flow has a higher velocity, and as a consequence, the $1/3$ velocity reduction is applied to a larger air-mass flowing through the rotor. The increase of velocity is directly related to the ratio β of the diffuser exit area A_3 with respect to the diffuser nozzle area A_1 as given in equation 2. Combining equation 1 and 2, the velocity V_1 in the nozzle of the diffuser can be expressed as a function of the free-stream velocity V_0 as in equation 3.

$$V_3 = (1 - a)V_0 \quad (1)$$

$$V_1 = \beta V_3 = \frac{A_3}{A_1} V_3 \quad (2)$$

$$V_1 = \beta(1 - a)V_0 \quad (3)$$

When the increased power is expressed as a power coefficient with respect to the rotor exit area, the maximum obtainable power coefficient of 0.59 still holds. However, when related to swept area of the rotor in the nozzle of the diffuser, the maximum C_P can surpass this value.

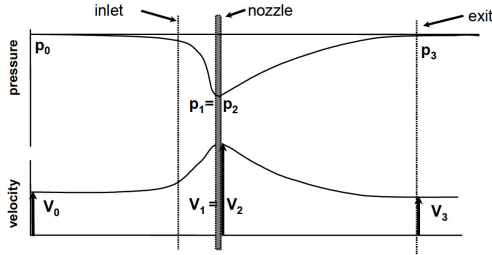


Figure 1: Pressure and velocity relations in an empty diffuser without back-pressure

Figure 1 shows the pressure and velocity for an empty diffuser without back-pressure. It is possible, however, that a back-pressure exists because of the Kutta condition, when the flow is forced to deflect in radial direction. As a result, the velocity at the exit of the empty diffuser V_3 can differ from the undisturbed flow velocity far in front of the diffuser V_0 as given in equation 4. The velocity increase results in a further augmentation of the power produced by a turbine placed in the nozzle of the diffuser.

$$V_3 = \gamma V_0 \quad (4)$$

The maximum achievable (ideal) power coefficient C_P can be expressed as in equation 5 or equation 6 when it is based on the rotor disc area or the diffuser exit area respectively.

$$C_{P_{rotor}} = \beta \gamma 4a(1 - a)^2 \quad (5)$$

$$C_{P_{exit}} = \gamma 4a(1 - a)^2 \quad (6)$$

2 Simulation Method

As explained by Simão Ferreira [2], the 1-D actuator disc model is not very well-suited for modeling a VAWT. However, it only assumes a pressure drop over the disc representing the energy extraction by the turbine and therefore it gives a rough indication of the theoretic maximum power increase as a result of a diffuser. Or in other

words: it provides a DAWT-equivalent of the well-known Betz-limit.

In order to evaluate the aerodynamic behavior of a VAWT and the effect of diffuser-augmentation, a 2-D simulation code is used. The code is an unsteady free-wake potential-flow panel model as described and used in [2]. It is this MATLAB-based program which is used to obtain the results displayed and discussed in the following sections. The blades and diffuser airfoils are modeled as doublet panels, while the wake is represented by free-moving singular vortex points.

3 Basic Vertical Axis Wind Turbine Operation

In steady operation, the aerodynamic loading on a VAWT is a periodic effect with the frequency of the rotation. This is much different from the steady operation of a HAWT, where the aerodynamic loading on the blades remains steady throughout the rotation. There are different ways to present the rotational variation of the loading on a VAWT since practically all output-variables experience related fluctuations. Figure 3 shows the instantaneous angle of attack experienced by a single blade over one rotor revolution. As a result of the continuously changing angle of attack, the forces on the blade change accordingly. In figure 4, the radial and tangential components of the force coefficients on one single blade are given. Time-dependent loading on the blade section causes the shedding of vorticity. As can be seen in figure 5, the shed vorticity obtains maximum strengths around azimuth positions of 35° (negative vorticity) and 170° (positive vorticity). The shed vorticity is transported into the wake, as visualized in figure 6. In figure 7, a flow field of streamlines is shown resulting from the time-averaged local velocities over one rotor revolution.

4 Diffuser-Augmented VAWT

In this section, the results from the previous section are compared with the simulation results of the same VAWT operating in the nozzle of a diffuser. For this general comparison, the area of the diffuser nozzle is equal to 1.6 times the diameter of the rotor.

The actual operation of the VAWT inside a diffuser varies little from the free-stream operation. The presence of the diffuser provides a flow acceleration through the rotor. With a fixed tip speed, the local angles of attack experienced by a blade during one revolution increase, as can clearly

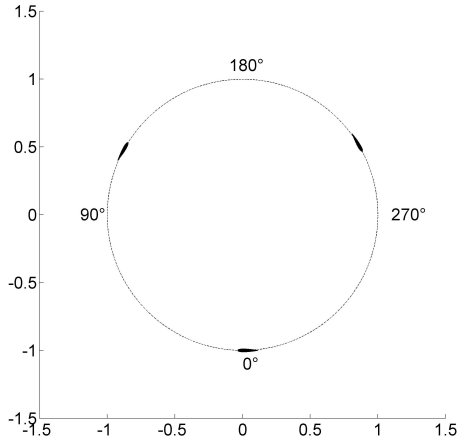


Figure 2: Azimuth position definition for a clockwise rotating VAWT

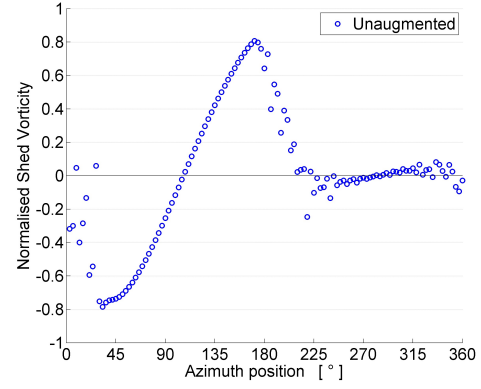


Figure 5: Normalized strength of the vorticity shed by a single blade per timestep ($\frac{\partial \Gamma_{wake}}{\partial \theta c \pi U_\infty}$)

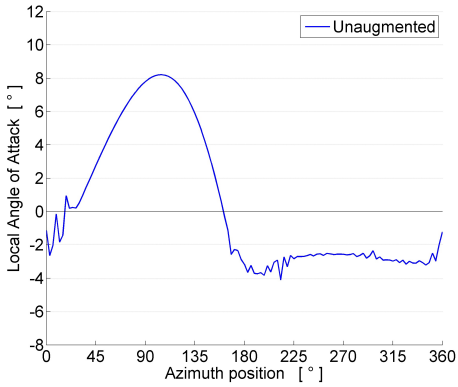


Figure 3: Phase-averaged angle of attack vs azimuthal position

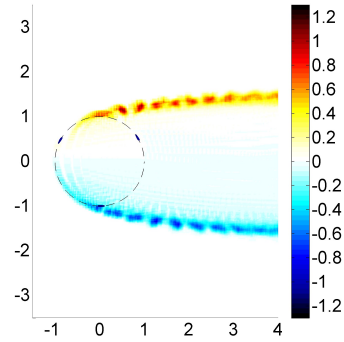


Figure 6: Phase-averaged vorticity distribution $\frac{\Gamma}{c^2 U_\infty}$ with the rotor at the zero azimuth position

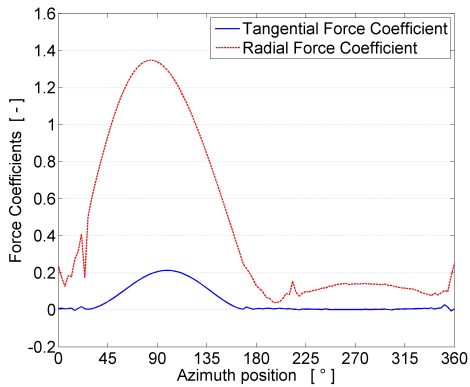


Figure 4: Instantaneous radial and tangential force coefficient of one single blade ($\frac{F}{\frac{1}{2} \rho \lambda^2 U_\infty^2 c}$)

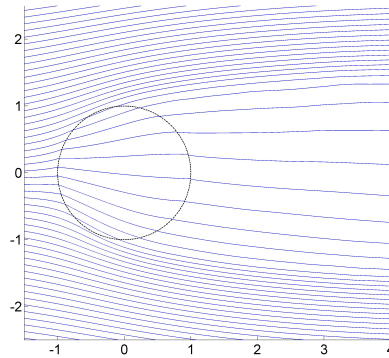


Figure 7: Streamlines visualizing the time-averaged local velocity field

be seen in figure 8. These higher absolute values for the angle of attack induce a higher blade loading, both in radial and in tangential direction. The dimensionless coefficients representing

these forces are given in figures 9 and 10. Note that the tangential force coefficient is positive in the direction of the rotation.

When looking at this tangential force coefficient, it is easy to see that there is a significant increase of rotor torque as a result of the diffuser. The time-

averaged power coefficient C_p for the diffuser-unaugmented turbine is 1.72 times as large as that of the un-augmented turbine. Which means an increase of about 72 percent. In order to make the comparison with the power increase as predicted by the 1-D actuator disc theory, the diffuser area ratio has to be evaluated. For the diffuser used here, the area ratio of the diffuser with respect to the nozzle is 1.76. This implies a 1-D prediction of power increase of 76 percent assuming no negative back-pressure.

This means the predicted power increase provided by the diffuser agrees almost perfectly with the obtained rise in power from the simulations. In order to validate the comparison made here, the same VAWT is next fitted with different diffusers, having different area ratios.

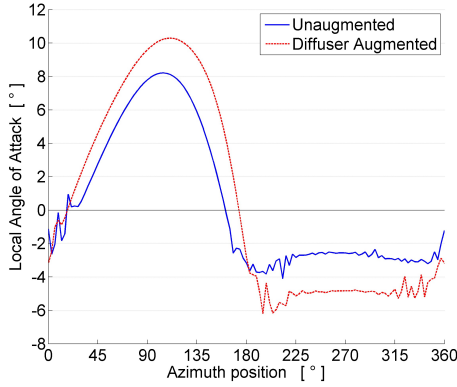


Figure 8: Angle of attack comparison between free and diffuser-augmented VAWT

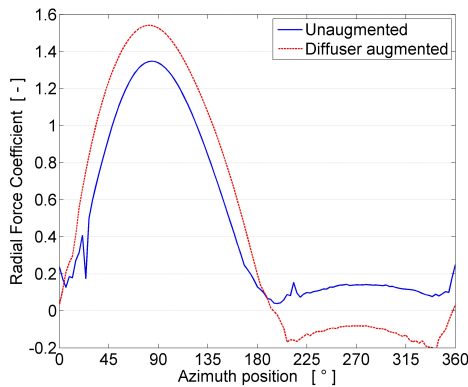


Figure 9: Radial force coefficient, contribution of one single blade ($\frac{F_R}{\frac{1}{2}\rho\lambda^2U_\infty^2c}$)

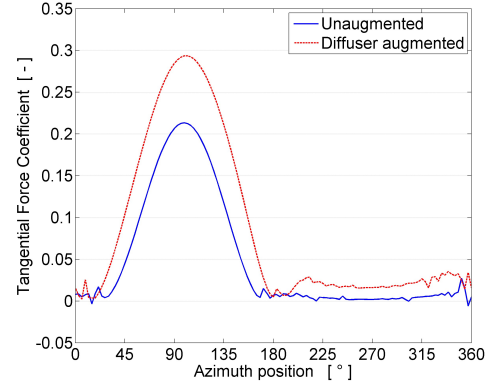


Figure 10: Tangential force coefficient, contribution of one single blade ($\frac{F_T}{\frac{1}{2}\rho\lambda^2U_\infty^2c}$)

5 Augmenting Effects of the Diffuser

The VAWT is simulated in combination with different diffuser areas. For every setup, the same cross-sectional shape is used for the diffuser. With the increasing nozzle area, the exit area ratio decreases, and since the diffuser is located further from the VAWT, its influence is expected to decrease. We look at the cases where the diffuser nozzle is 1.2, 1.4, 1.6, 1.8 and 2 times the diameter of the turbine. Four of these setups are shown in figure 11. The tangential force coefficient for all the above-mentioned cases is shown in figure 12. The average power coefficient C_p can be expressed relative to the power coefficient of the unaugmented VAWT, as is given in table 1 along with the ratio β of the diffuser exit area with respect to the nozzle area. As can clearly be concluded from table 1, there is hardly any torque increase as a result of the 1.2R-diffuser with the highest area ratio β . This fact suggests that the area ratio is not the driving factor in the diffuser-augmented operation of the VAWT, and the good agreement of augmentation factors in the previous section can be considered to be a lucky shot.

Table 1: Comparison of diffuser exit area ratio β and relative power coefficient $\frac{C_p}{C_{p0}}$ with C_{p0} the power coefficient of the unaugmented turbine

A_{nozzle}	β	relative C_p
No Diffuser	-	1
1.2R	2	1.06
1.4R	1.87	1.23
1.6R	1.76	1.72
1.8R	1.67	1.66
2R	1.61	1.80

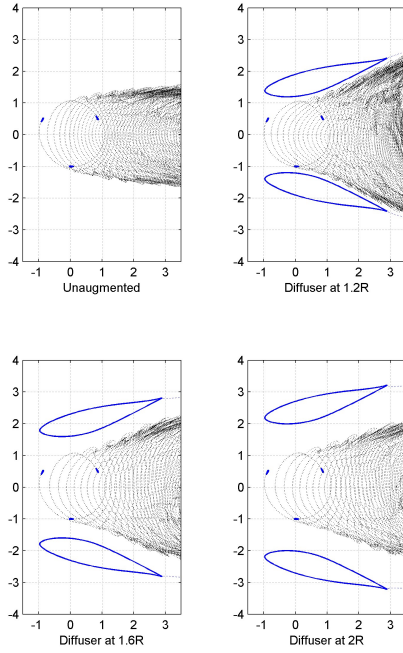


Figure 11: Visualization of the VAWT-diffuser combination for four of the simulated cases

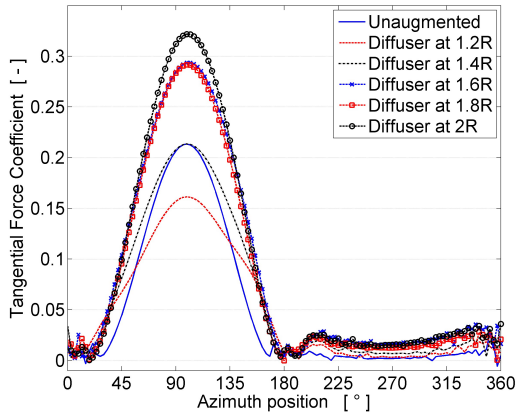


Figure 12: Torque coefficient contribution of single blade for different diffuser nozzle areas $\left(\frac{F_T}{\frac{1}{2}\rho\lambda^2U_\infty^2c}\right)$

From the torque-contribution of a single blade in figure 12, it is possible to see that there is a drop in the peak of the tangential force around the azimuth position of 100° for the $1.2R$ diffuser case. Also, there is a gain around 35° and 160° . These phases of power gain cancel out with the drop of the power peak, resulting in almost the same average power coefficient C_p over a full rotation as the unaugmented turbine (see table 1).

With increasing diffuser nozzle area, the decrease of the peak in the tangential force coefficient plot at 100° transforms into an increase with respect to the unaugmented case providing a steady rise of the torque at all azimuth positions. This trend also shows when looking at the local angle of attack in figure 13.

In order to understand what is happening, we should take a look at the local velocity of the flow through the rotor. Figures 14 and 15 show the local time-averaged induction $a = 1 - \frac{U_x}{U_\infty}$ in the direction of the free-stream flow. The large local angle of attack in the case of the $1.6R$ diffuser is caused by a higher incoming flow velocity at the rotor. This is a striking observation, since the velocity increase inside the empty $1.2R$ diffuser is expected to be higher than that of the $1.6R$ diffuser. This clearly means that the prediction of maximum achievable power increase by the 1-D actuator disc theory does not hold for a diffuser-augmented VAWT. The reason for this can be found in the gap between the inside of the diffuser-nozzle and the turbine. For the diffuser with the $1.2R$ nozzle section, there is practically no gap. The shape of the diffuser airfoil causes the peak in the local angle of attack to occur earlier in the rotation, and to remain until a later azimuth position than the unaugmented turbine. This is due to the local flow direction rather than due to the local flow velocity. This directional difference near the azimuth positions of 35° and 160° is visible when comparing the unaugmented flow field in figure 7 with the augmented flow field in figure 16. The change in shape of the load-peak in the up-wind part of the rotation also has consequences for the shedding of the vorticity. Figure 17 shows that the peak of the shed vorticity of the $1.2R$ diffuser is higher and occurs in a shorter time-span then for the unaugmented turbine. The stronger and more concentrated vortices that are shed result in a stronger induction. Around the 90° azimuth position, the increased induction reduces the local flow velocity, and thus decreases the local angle of attack experienced by the blades. This explains the power loss which can be seen as the lower tangential force peak in figure 12 with respect to the unaugmented case.

But then why does this not happen in the same way when a larger diffuser-nozzle is applied? The answer to this question might be found in the representations of the vorticity distribution. Figures 18 and 19 show the distribution of vorticity for the $1.2R$ and the $1.6R$ diffuser respectively. For the $1.6R$ diffuser, due to the faster-moving flow just outside the rotor, the concentrated vortices which

are shed with every blade passing are transported faster downwind. The amount of vorticity shed per blade passage in this case is also larger as could be seen in figure 17. This larger vortex strength has a stronger induction at the rotor as a consequence. However, the effect of a faster vortex-movement in the case of the $1.6R$ has a stronger influence. When the shed vortices are further away from the rotor, they induce less velocity decrease at the rotor, allowing for higher positive angles of attack at the upwind blade positions and negative angles at the downwind blade positions, both resulting in a larger torque on the rotor over the whole rotation.

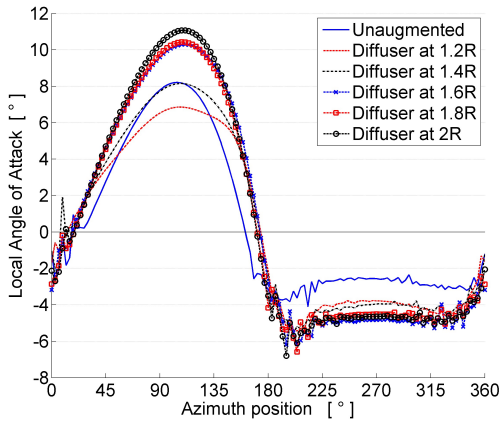


Figure 13: Local angle of attack for different diffuser nozzle areas

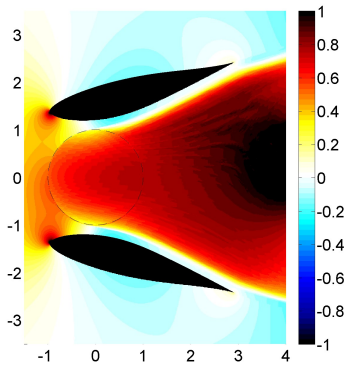


Figure 14: Time-averaged local velocity induction $a = 1 - \frac{U_x}{U_\infty}$ for the VAWT operating inside the $1.2R$ diffuser

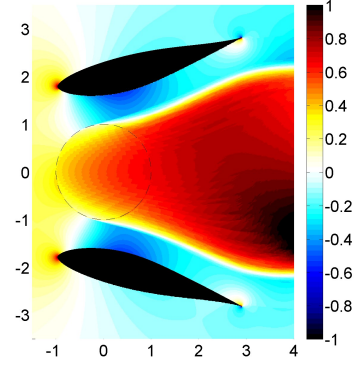


Figure 15: Time-averaged local velocity induction $a = 1 - \frac{U_x}{U_\infty}$ for the VAWT operating inside the $1.6R$ diffuser

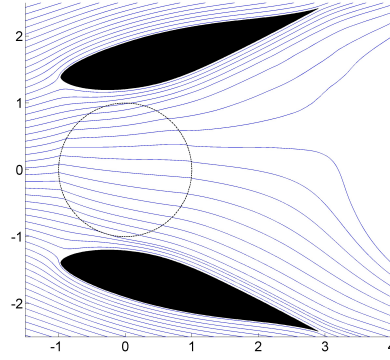


Figure 16: Streamlines visualizing the time-averaged local velocity field

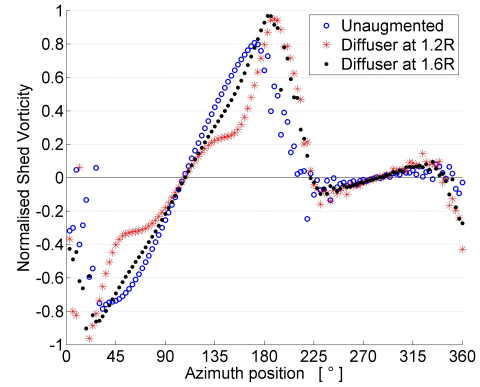


Figure 17: Normalized strength of the shed vorticity of a single blade $(\frac{\partial \Gamma_{wake}}{\partial \theta c \pi U_\infty})$

6 Conclusions and Further Investigations

For the evaluation of diffuser-augmented horizontal axis wind turbines (DAWT's), a 1-D actuator

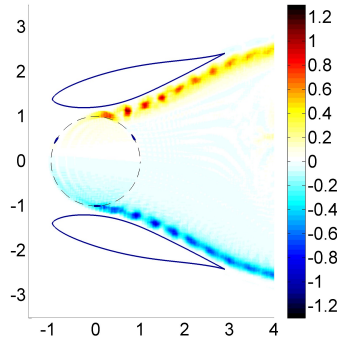


Figure 18: Phase-averaged vorticity distribution $\frac{\Gamma}{c^2} \frac{c}{U_\infty}$ with the rotor at the zero azimuth position inside the $1.2R$ diffuser

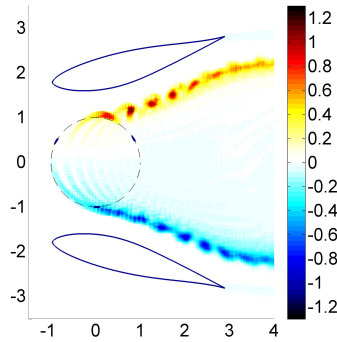


Figure 19: Phase-averaged vorticity distribution $\frac{\Gamma}{c^2} \frac{c}{U_\infty}$ with the rotor at the zero azimuth position inside the $1.6R$ diffuser

disc theory can be used linking the theoretical maximum power increase of the DAWT to the velocity increase produced by the empty diffuser. The velocity increase, and thus also the power increase, can be directly expressed as the ratio of the exit area of the diffuser with respect to the nozzle area of the diffuser. Although not perfectly suitable for application to a vertical axis wind turbine (VAWT), this 1-D approach can serve as a reference for the expected power increase. From initial simulations with a nozzle area of 1.6 times the rotor diameter, it can be seen that the power increase of the VAWT nicely fits the increase predicted by the 1-D actuator theory. As is shown by varying the nozzle area (1.2, 1.4, 1.6, 1.8 and 2 times the rotor diameter), the amount of power increase is dependent on the size of the gap between the rotor and the diffuser. The high-velocity flow outside the rotor will transport the shed vorticity away from the rotor, reducing the local induction at the blade positions. The lower local induction allows for larger local angles

of attack, providing more torque. Thus, rather than the area ratio of the diffuser itself (and thus the velocity increase produced by the empty diffuser) it is the size of the gap between the rotor and the diffuser that effects the power augmentation of the diffuser-augmented VAWT. In that context, the work of Aquiló et al ([1]) should be revisited. Aquiló et al use CFD-calculations to predict the (1-D) speed-up of the flow through a building-augmented wind concentrator. For the application of HAWTs, this estimation might prove valid, but when this approach is used to estimate the expected power augmentation of a VAWT placed inside this wind concentrator system, the result may become invalid.

Even though the presented aerodynamic investigation gives a clear explanation for the occurring phenomena, it is considered that other aerodynamic effects might play a role in reducing or enhancing the explained effects. To this extend, more effort is needed in order to investigate other possible effects influencing the performance of the augmented VAWT. Since the area ratio of the diffuser is not the driving factor in the augmentation, a whole different diffuser setup should be considered. On the other hand, the above conclusions should be checked and proven using other simulation methods and experimental research.

References

- [1] A. Aguilo, D. Taylor, A. Quinn, and R. Wiltshire. Computational fluid dynamic modelling of windspeed enhancement through a building-augmented wind concentration system. *EWE Conference 2004 - Poster Presentation*, 2004.
- [2] Carlos Simão Ferreira. *The near wake of the VAWT*. PhD thesis, Faculty of Aerospace Engineering, Delft University of Technology, 2009.
- [3] Gerard J. W. van Bussel. An assessment of the performance of diffuser augmented wind turbines (dawt's). *3rd ASME/JSME Fluid Engineering Conference FEDSM99-7830, San Francisco, USA*, 1999.
- [4] Gerard J. W. van Bussel. The science of making more torque from wind: Diffuser experiments and theory revisited. *The Science of Making Torque from Wind, Journal of Physics: Conference Series 75*, 2007.